Turkish Journal of Electrical Engineering & Computer Sciences

http://journals.tubitak.gov.tr/elektrik/

Research Article

Turk J Elec Eng & Comp Sci
(2017) 25: 4486 – 4495

doi:10.3906/elk-1705-153

Analysis and design of an invisibility cloak based on transformation optics at microwave frequencies

Maryam BAYATI*, Masood OMOOMI
Department of Electrical and Computer Engineering, Isfahan University of Technology, Isfahan, Iran

Received: 13.05.2017 • **Accepted/Published Online:** 15.09.2017 • **Final Version:** 03.12.2017

Abstract: Invisibility cloaks can be constructed with electromagnetic metamaterials. In this paper, structural metamaterials are used to design an invisibility cloak. To this end, transformation optics is used to design electromagnetic parameters. These parameters are selected so that when we excite the cloak its presence does not perturb radiated fields. Therefore, we formulate the electric field both at the inner and outer parts of the cloak, when the excitation source is placed both inside and outside, and we show that the scattered fields will be suppressed due to its presence. Finally, simulation results verify that the invisibility cloak is well designed and is able to hide the cylindrical metal inside it.

Key words: Cloak, invisibility, transformation optics, cylindrical metal

1. Introduction

After the first double negative materials experiment, research on metamaterials has increased. The transformation optics theory proposes a complete tool for using vast facilities about metamaterials constitutive parameters. Many interesting optical devices have been recognized, especially the invisibility cloak. Metamaterials gain their features from their unit structures. The unit cell dimensions in a metamaterial must be smaller than the operating wavelength [1]. This condition will guarantee the homogeneity of the overall material at a macroscopic scale. In transformation optics, two spaces, namely physical and virtual, must be considered. This theory describes the relation between the electromagnetic features of two spaces such as fields, charge densities, and dielectric constants [2,3]. Recently, the interior invisibility cloak has been taken into account by the transformation optics. In this type of cloak, the transfer function occurs in a way that it transforms the entire virtual space into a part of the physical space, so that some points in the physical space will exist where no projection exists for them in the virtual space. Various methods have been proposed for designing an invisibility cloak with an unconventional shape, based on transformation theory. Yan et al. [4] theoretically analyzed the wave properties in the cloak boundary and verified that it is possible to make an arbitrary invisibility cloak. Jiang et al. [5] utilized nonuniform function to describe the geometrical boundary of an invisibility cloak with unconventional shape and obtain the medium parameters. Moreover, Nicolet et al. [6] used the finite Fourier expansion method to specify random boundaries, whose medium properties were calculated after gaining the Fourier expansion of the boundary. In this paper, we investigate wave propagation in the optical metamaterials that have anisotropic constitutive parameters. The required dielectric properties for these metamaterials have been extracted using transformation optics. Based on Maxwell's equations and a linear electric line source as incident wave, the scattering fields must be zero due to the existence of the ideal cloak. Finally, the invisibility cloak is simulated

*Correspondence: m.bayati@ec.iut.ac.ir

by employing COMSOL multiphysics. The next section explains the theoretical formulation for the scattered fields inside and outside the cloak. Section 3 performs the cloak simulation based on finite element solver, COMSOL multiphysics. Finally, Section 4 presents the conclusions.

2. Electric field inside and outside the cloak

This section introduces the required wave equations that describe the invisibility cloak. The cloak is excited by an infinite line source and formulates the electric field inside and outside. Two cases are examined, i.e. the infinite line source is placed inside and outside the cloak. Ideally, the observation point outside the cloak will not sense the cylindrical metal inside it, if its presence does not perturb the radiated field.

2.1. Wave equation in the cylindrical cloak

A cylindrical cloak, based on coordinate transformation, is shown in Figure 1. This type of cloak is created by using a coordinate transformation as follows:

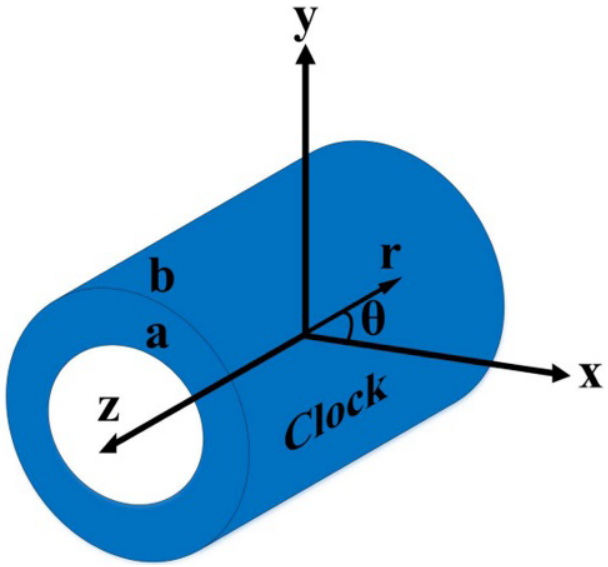

Figure 1. Ideal infinite cylindrical cloak.

$$r \rightarrow \frac{b-a}{b}r + a, \quad \theta \rightarrow \theta, \quad z \rightarrow z \tag{1}$$

This transformation transforms the cylindrical region $0 < r < b$ to the annular region $a < r < b$, where a and b are the inner and outer radii of the cylindrical cloak, respectively. According to the invariant form of Maxwell's equations with respect to coordinate transformations, only the permittivity and permeability tensors are affected by these transformations. Therefore [7],

$$\varepsilon_r = \mu_r = \frac{h_\theta h_z}{h_r} = \frac{r-a}{r} \tag{2a}$$

$$\varepsilon_\theta = \mu_\theta = \frac{h_r h_z}{h_\theta} = \frac{r}{r-a} \tag{2b}$$

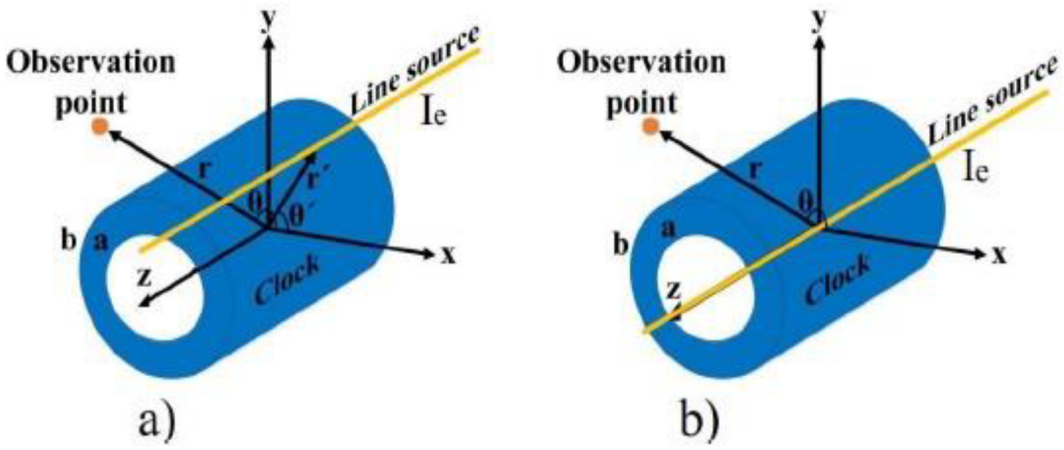

Figure 2. Infinite cylindrical cloak with the infinite electric line source: a) outside, and b) inside.

$$\varepsilon_z = \mu_z = \frac{h_r h_\theta}{h_z} = \left(\frac{b}{b-a}\right)^2 \frac{r-a}{r} \tag{2c}$$

The mentioned parameters construct the diagonal entries of permittivity and permeability tensors, and the rest of the entries are zero. To extract wave equation in the region of the invisibility cloak, we use source-free Maxwell's equations:

$$\nabla \times \vec{E} = -j\omega\overline{\overline{\mu}}.\vec{H} \tag{3a}$$

$$\nabla \times \vec{H} = j\omega\overline{\overline{\varepsilon}}.\vec{E} \tag{3b}$$

By combining the above curl equations, an equation is obtained that only has the electric field as follows:

$$\vec{E} = \frac{1}{j\omega}\overline{\overline{\varepsilon}}^{-1}\left\{\nabla \times \left[\frac{1}{-j\omega}\overline{\overline{\mu}}^{-1}\left(\nabla \times \vec{E}\right)\right]\right\} \tag{4}$$

Therefore, the wave equation inside the cloak is

$$\nabla \times \left[\overline{\overline{\mu}}^{-1}\left(\nabla \times \vec{E}^{\,c}\right)\right] - \omega^2\overline{\overline{\varepsilon}}\vec{E}^{\,c} = 0, \tag{5}$$

where $\vec{E}^{\,c}$ is the electric field inside the cloak. Here we only investigate the case of TM^z polarization. By referring to Eq. (1) and using the electromagnetic duality that held between fields and constitutive parameters, we can obtain a magnetic field wave equation for the case of TE^z polarization. Therefore, the behavior and performance of the invisibility cloak are independent of incident field polarization. For TM^z polarization, which deals only with the electric field, Eq. (5) is reduced to the following form:

$$r^2\frac{\partial^2 E_z^c}{\partial r^2} + r\mu_\theta\frac{\partial E_z^c}{\partial r} + \frac{\mu_\theta}{\mu_r}\frac{\partial^2 E_z^c}{\partial \theta^2} + \varepsilon_z\mu_\theta r^2\beta_0^2 E_z^c = 0, \tag{6}$$

where β_0 is free space wavenumber, and we see that only ε_z, μ_r, and μ_θ are relevant in the wave equation of E_z^c. By substituting the associated parameters of the ideal cloak in Eq. (2), the wave equation will have the

following form:

$$r^2\frac{\partial^2 E_z^c}{\partial r^2}+\frac{r^2}{r-a}\frac{\partial E_z^c}{\partial r}+\frac{r^2}{(r-a)^2}\frac{\partial^2 E_z^c}{\partial \theta^2}+\left(\frac{b}{b-a}\right)^2 r^2\beta_0^2 E_z^c=0 \tag{7}$$

Using the separation variables method, E_z^c is factorized as

$$E_z^c(r,\theta,z)=E_z^c(r).E_z^c(\theta).E_z^c(z) \tag{8}$$

Regarding $E_z^c(\theta)=e^{jn\theta}$ and $E_z^c(z)=e^{j\beta_z z}$, one can find $E_z^c(r)$ by solving the following n-order Bessel differential equation [8]:

$$(r-a)^2\frac{d^2E_z^c(r)}{dr^2}+(r-a)\frac{dE_z^c(r)}{dr}+\left[\left(\frac{b}{b-a}\right)^2(r-a)^2\beta_0^2-n^2\right]E_z^c(r)=0 \tag{9}$$

The general solution of (9) is $f_n[\beta_r(r-a)]$, where $\beta_r=\beta_0 b/(b-a)$ and f_n is Bessel or Hankel function of order n. Therefore, the electric field inside the invisibility cloak can be written as follows:

$$E_z^c(r,\theta,z)=\sum_{n=-\infty}^{+\infty}\left\{\alpha_n^{c_1}J_n[\beta_r(r-a)]+\alpha_n^{c_2}H_n^{(1)}[\beta_r(r-a)]\right\}e^{jn(\theta)+j\beta_z z} \tag{10}$$

where $\alpha_n^{c_1}$ and $\alpha_n^{c_2}$ are unknown coefficients of the expansion for the electric fields inside the ideal cloak, which must be determined, and J_n and $H_n^{(1)}$ are the n-order Bessel and Hankel functions of the first type, respectively.

2.2. Near field formulation

In this section, we extract the electric field in different regions. Figure 2a shows a cylindrical cloak that is located along the z-axis with an outer radius b and inner radius a. We assume that regions $r<a$ and $r>b$ are free space. The infinite electric line source is located outside and inside the cloak at r', as shown in Figures 2a and 2b, respectively. The radiated fields only have the TM^z mode, because the infinite line source is located along the z-axis. Hence, we can write the z component of the incident electric field as the following equation [8]:

$$E_z^i(r,\theta)=-\frac{\beta_0^2 I_e}{4\omega\varepsilon_0}\begin{cases}\sum\limits_{n=-\infty}^{\infty}J_n(\beta_0 r)H_n^{(2)}(\beta_0 r')e^{jn(\theta-\theta')} & r\le r'\\ \sum\limits_{n=-\infty}^{\infty}J_n(\beta_0 r')H_n^{(2)}(\beta_0 r)e^{jn(\theta-\theta')} & r\ge r'\end{cases} \tag{11}$$

Firstly, we examine the structure shown in Figure 2a. In this situation, the electric field in different regions can be expressed as in [8]:

$$E_z^{int}(r,\theta)=\left(-\frac{\beta_0^2 I_e}{4\omega\varepsilon_0}\right)\sum\nolimits_{n=-\infty}^{\infty}\left[A_n^{int}J_n(\beta_0 r)\right]e^{jn(\theta-\theta')} \qquad r\le a \tag{12}$$

$$E_z^c(r,\theta)=\left(-\frac{\beta_0^2 I_e}{4\omega\varepsilon_0}\right)\sum\nolimits_{n=-\infty}^{\infty}\left\{A_n^{c_1}J_n[\beta_r(r-a)]+A_n^{c_2}H_n^{(1)}[\beta_r(r-a)]\right\}e^{jn(\theta-\theta')} \quad a\le r\le b \tag{13}$$

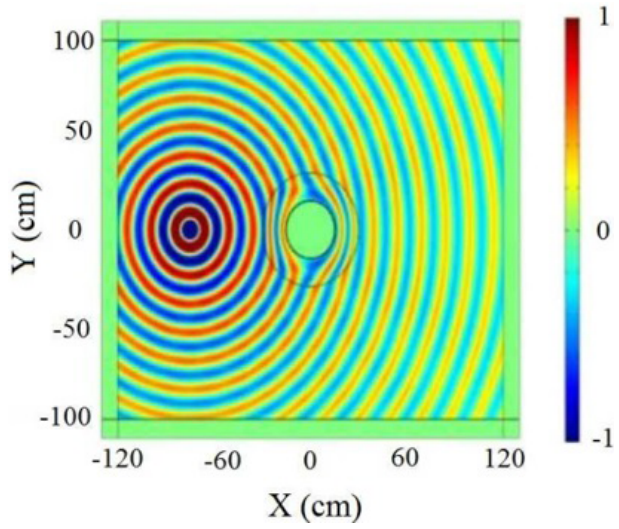

Figure 3. Simulation results based on full-wave solver when the incident wave is located outside the cloak.

$$E_z^s(r,\theta) = \left(-\frac{\beta_0^2 I_e}{4\omega\varepsilon_0}\right)\sum_{n=-\infty}^{\infty}\left[A_n^s H_n^{(2)}(\beta_0 r)\right]e^{jn(\theta-\theta')} \qquad r \geq b \tag{14}$$

The total electric field outside the cloak can be expressed by the sum of incident and scattered electric fields [9]:

$$E_z^{out}(r,\theta) = E_z^i(r,\theta) + E_z^s(r,\theta) = -\frac{\beta_0^2 I_e}{4\omega\varepsilon_0}\begin{cases}\sum\limits_{n=-\infty}^{\infty}\left[J_n(\beta_0 r)H_n^{(2)}(\beta_0 r') + A_n^s H_n^{(2)}(\beta_0 r)\right]e^{jn(\theta-\theta')} & b \leq r \leq r' \\ \sum\limits_{n=-\infty}^{\infty}\left[J_n(\beta_0 r') + A_n^s\right]H_n^{(2)}(\beta_0 r)\,e^{jn(\theta-\theta')} & r \geq r'\end{cases} \tag{15}$$

Due to the existence of the perfect electric conductor in region $r \leq a$, the electromagnetic fields will vanish in this region. According to Maxwell's equations and Faraday's law, the magnetic field can be obtained as follows:

$$\vec{H}(r,\theta) = \frac{1}{-j\omega\mu_0}\left[\nabla \times \vec{E}(r,\theta)\right] \tag{16}$$

For TM^z polarization, the electric field has only z component. As a result, the magnetic field only has r and θ components. Using Eq. (16), the θ component of the magnetic field inside and outside the cloak is as follows:

$$\begin{aligned} H_\theta^{out}(r,\theta) &= \frac{1}{j\omega\mu_0}\frac{\partial E_z^{out}}{\partial r} \\ &= j\frac{\beta_0 I_e}{4}\begin{cases}\sum\limits_{n=-\infty}^{\infty}\left[J_n'(\beta_0 r)H_n^{(2)}(\beta_0 r') + A_n^s H_n^{(2)'}(\beta_0 r)\right]e^{jn(\theta-\theta')} & b \leq r \leq r' \\ \sum\limits_{n=-\infty}^{\infty}\left[J_n(\beta_0 r') + A_n^s\right]H_n^{(2)'}(\beta_0 r)\,e^{jn(\theta-\theta')} & r \geq r'\end{cases}\end{aligned} \tag{17}$$

$$H_{\theta}^{c}(r,\theta) = \frac{1}{j\omega\mu_0\mu_{\theta}}\frac{\partial E_z^c}{\partial r}$$
$$= j\frac{\beta_r I_e}{4\mu_{\theta}}\sum_{n=-\infty}^{\infty}\left\{A_n^{c_1}J_n'[\beta_r(r-a)]+A_n^{c_2}H_n^{(1)'}[\beta_r(r-a)]\right\}e^{jn(\theta-\theta')} \quad a\le r\le b \tag{18}$$

The unknown coefficients A_n^{int}, $A_n^{c_1}$, $A_n^{c_2}$, and A_n^{s} are found by applying boundary conditions to calculate the electric field in different regions. The unknown coefficients are found by applying boundary conditions on cylindrical surfaces and then performing algebraic operations, as well as considering the limitations of the Bessel function when its argument approaches zero.

To avoid divergence and provide singularity in Eq. (3b), we assume that the interior boundary of the cloak has been located at $r=a+\delta$, and then δ gradually approaches zero in the related equations [10]. By applying boundary condition on the inner boundary $r=a$, which is the conductor surface, we have

$$E_z^c(a,\theta)=0 \Longrightarrow A_n^{c_1}J_n[\beta_r(\delta)]+A_n^{c_2}H_n^{(1)}[\beta_r(\delta)]=0 \tag{19}$$

In the same manner, by applying the boundary condition on the outer boundary $r=b$, we have

$$E_z^{out}(b,\theta)=E_z^c(b,\theta)\Longrightarrow J_n(\beta_0 b)H_n^{(2)}(\beta_0 r')+A_n^s H_n^{(2)}(\beta_0 b)= A_n^{c_1}J_n[\beta_r(b-a)]+A_n^{c_2}H_n^{(1)}[\beta_r(b-a)] \tag{20}$$

$$H_{\theta}^{out}(b,\theta)=H_{\theta}^{C}(b,\theta)\Longrightarrow \beta_0\left[J'_n(\beta_0 b)H_n^{(2)}(\beta_0 r')+A_n^s H_n^{'(2)}(\beta_0 b)\right]$$
$$=\frac{\beta_r}{\mu_{\theta(b)}}\left\{A_n^{c_1}J_n'[\beta_r(b-a)]+A_n^{c_2}H_n^{'(1)}[\beta_r(b-a)]\right\} \tag{21}$$

In Eq. (19), when $\delta\to 0$, the argument of the Hankel function approaches zero. Therefore, to avoid the right-hand side of Eq. (19) becoming infinite, coefficient $A_n^{c_2}$ must be equal to zero. In Eq. (21), we can write coefficient $\frac{\beta_r}{\mu_{\theta(b)}}$ as follows:

$$\frac{\beta_r}{\mu_{\theta(b)}}=\frac{\beta_0\frac{b}{b-a}}{\frac{b}{b-a}}=\beta_0 \tag{22}$$

Then coefficients A_n^s and $A_n^{c_1}$ can be calculated as follows:

$$A_n^s=H_n^{(2)}(\beta_0 r')\times\frac{J_n(\beta_0 b)J_n'[\beta_r(b-a)]-J_n'(\beta_0 b)J_n[\beta_r(b-a)]}{J_n[\beta_r(b-a)]H_n^{'(2)}(\beta_0 b)-J_n'[\beta_r(b-a)]H_n^2(\beta_0 b)} \tag{23a}$$

$$A_n^{c_1}=-H_n^{(2)}(\beta_0 r')\times\frac{J_n'(\beta_0 b)H_n^{(2)}(\beta_0 b)-J_n(\beta_0 b)H_n^{'(2)}(\beta_0 b)}{J_n'[\beta_r(b-a)]H_n^{(2)}(\beta_0 b)-J_n[\beta_r(b-a)]H_n^{'(2)}(\beta_0 b)} \tag{23b}$$

With regards to $\beta_0 b=\beta_r(b-a)$, the nominator of Eq. (23a) becomes zero. As a result, coefficient A_n^s must be zero too.

$$A_n^{int}=0,\quad A_n^{c_2}=0,\quad A_n^s=0 \tag{24}$$

By using Eq. (20), coefficient $A_n^{c_1}$ is calculated according to the following equation:

$$A_n^{c_1}=H_n^{(2)}(\beta_0 r') \tag{25}$$

Therefore, in the ideal cloak there is no scattering field outside. Additionally, the waves inside the cloak with related propagation constant propagate similarly to the waves in the free space outside the cloak. As a result, the presence of the cylindrical conductor is not sensed. This shows that the scattering fields from the cloak are zero when the incident wave impinges on its outside.

Secondly, the electric field is calculated for the structure shown in Figure 2b. As described above, the electric field inside the cloak, $r < a$, can be calculated as

$$E_z^{int}(r,\theta) = E_z^i(r,\theta) + \left(-\frac{\beta_0^2 I_e}{4\omega\varepsilon_0}\right)\sum_{n=-\infty}^{\infty}\alpha_n^{int} J_n(\beta_0 r)\, e^{jn(\theta-\theta')} \tag{26}$$

According to Eq. (10), the electric field in the cloak region, i.e. $a < r < b$, will be as follows:

$$E_z^c(r,\theta) = \left(-\frac{\beta_0^2 I_e}{4\omega\varepsilon_0}\right)\sum_{n=-\infty}^{\infty}\left\{\alpha_n^{c_1} J_n[\beta_r(r-a)] + \alpha_n^{c_2} H_n^{(1)}[\beta_r(r-a)]\right\} e^{jn(\theta-\theta')} \tag{27}$$

Finally, the electric field in the exterior region, i.e. $r > b$, can be described as

$$E_z^{out}(r,\theta) = \left(-\frac{\beta_0^2 I_e}{4\omega\varepsilon_0}\right)\sum_{n=-\infty}^{\infty}\alpha_n^{out} H_n^{(2)}(\beta_0 r)\, e^{jn(\theta-\theta')} \tag{28}$$

The four unknown coefficients α_n^{int}, $\alpha_n^{c_1}$, $\alpha_n^{c_2}$, and α_n^{out}, used to calculate the electric field in different regions, are obtained by applying boundary conditions to the two surfaces $r = a$ and $r = b$. By applying boundary conditions to the interior boundary $r = a$, which is the conducting surface, we have

$$J_n(\beta_0 r') H_n^{(2)}[\beta_0(a+\delta)] + \alpha_n^{int} J_n[\beta_0(a+\delta)] = \alpha_n^{c_1} J_n(\beta_r\delta) + \alpha_n^{c_2} H_n^{(1)}(\beta_r\delta) \tag{29}$$

$$\beta_0 Jn(\beta_0 r') H_n^{'(2)}[\beta_0(a+\delta)] + \beta_0\alpha_n^{int} J_n'[\beta_0(a+\delta)] = \frac{\beta_r}{\mu_{\theta(a+\delta)}}\alpha_n^{c_1} J_n'(\beta_r\delta) + \frac{\beta_r}{\mu_{\theta(a+\delta)}}\alpha_n^{c_2} H_n^{'(1)}(\beta_r\delta) \tag{30}$$

In the same manner, by applying boundary conditions to the exterior boundary $r = b$, the following equation can be obtained:

$$\alpha_n^{out} H_n^{(2)}(\beta_0 b) = \alpha_n^{c_1} J_n[\beta_r(b-a)] + \alpha_n^{c_2} H_n^{(1)}[\beta_r(b-a)] \tag{31}$$

$$\beta_0\alpha_n^{out} H_n^{'(2)}[\beta_0(a+\delta)] = \frac{\beta_r}{\mu_{\theta(b)}}\alpha_n^{c_1} J_n'[\beta_r(b-a)] + \frac{\beta_r}{\mu_{\theta(b)}}\alpha_n^{c_2} H_n^{'(1)}[\beta_r(b-a)] \tag{32}$$

Using Eqs. (17)–(19), and considering the Wronskian of Bessel functions, the unknown coefficients of the expansion can be found as in [8]:

$$\alpha_n^{int} = -J_n(\beta_0 r') \times \frac{\left[\frac{b\delta}{a(b-a)}\frac{H_n^{'(2)}\left(\beta_0\frac{b}{b-a}\delta\right)}{H_n^{(2)}\left(\beta_0\frac{b}{b-a}\delta\right)} H_n^{(2)}(\beta_0 a) - H_n^{'(2)}(\beta_0 a)\right]}{\left[\frac{b\delta}{a(b-a)}\frac{H_n^{'(2)}\left(\beta_0\frac{b}{b-a}\delta\right)}{H_n^{(2)}\left(\beta_0\frac{b}{b-a}\delta\right)} J_n(\beta_0 a) - J_n'(\beta_0 a)\right]} \tag{33}$$

$$\alpha_n^{out} = -\frac{J_n(\beta_0 a)}{H_n^{(2)}\left(\beta_0 \frac{b}{b-a}\delta\right)} \times J_n(\beta_0 r') \times \frac{\left[\frac{b\delta}{a(b-a)} \frac{H_n^{'(2)}\left(\beta_0 \frac{b}{b-a}\delta\right)}{H_n^{(2)}\left(\beta_0 \frac{b}{b-a}\delta\right)} H_n^{(2)}(\beta_0 a) - H_n^{'(2)}(\beta_0 a)\right]}{\left[\frac{b\delta}{a(b-a)} \frac{H_n^{'(2)}\left(\beta_0 \frac{b}{b-a}\delta\right)}{H_n^{(2)}\left(\beta_0 \frac{b}{b-a}\delta\right)} J_n(\beta_0 a) - J'_n(\beta_0 a)\right]}$$
$$+\frac{H_n^{(2)}(\beta_0 a)}{H_n^{(2)}\left(\beta_0 \frac{b}{b-a}\delta\right)} J_n(\beta_0 r') \tag{34}$$

$$\alpha_n^{c_1} = 2\alpha_n^{out}, \quad \alpha_n^{c_2} = -\alpha_n^{out} \tag{35}$$

Based on the above equations, we conclude that when $\delta \to 0$ approaches zero, the denominator of Eq. (34) approaches infinity, whereas its nominator remains bounded. Therefore, coefficient α_n^{out} approaches zero, and in Eq. (35) coefficients $\alpha_n^{c_1}$ and $\alpha_n^{c_2}$ approach zero as well. As a result, when the line source is located in region $r < a$, no field exists inside the cloak layer nor outside it. Therefore, when the linear line source is located inside the cloak, no field will leak outside it.

3. Simulation results

In this section, we validate of the results obtained from the previous section by simulating the cloak structure using the COMSOL full-wave simulator, which works based on the finite element method. In this simulation, we assume that the operating frequency is 2 GHz, and the cloak inner and outer radius are $a = \lambda_0$ and $b = 2\lambda_0$, respectively. Therefore, the cloak will have one wavelength thickness. In the case of exterior illumination, a linear line source is located at a distance of two times the wavelength from the cloak exterior boundary. In the other configuration, a linear source is located along the cloak axis [11]. In this simulation, we have used finer mesh for cylindrical finite layer with inner radius a and outer radius $a + \delta$, where $\delta = 5$ mm, so that the impact of the permeability and permittivity tensors related to the ideal cloak on the boundary can be seen more clearly. Therefore, for this region, a maximum mesh size of 1 mm is considered. The simulation result is shown in Figure 3. We can see that great agreement exists between the theoretical and simulation results, and the

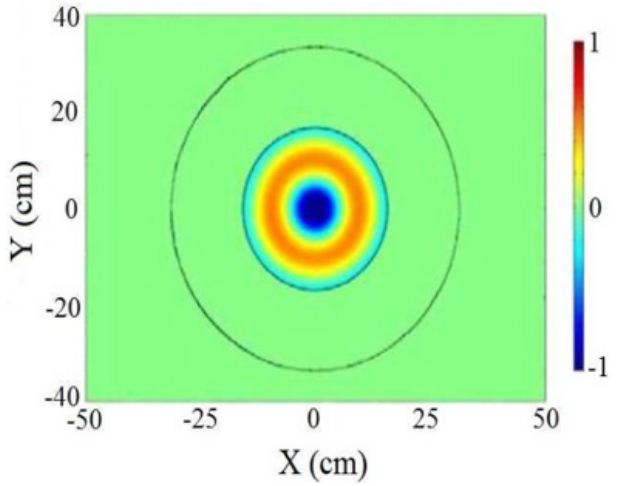

Figure 4. Simulation results based on full-wave solver when the incident wave is located inside the cloak.

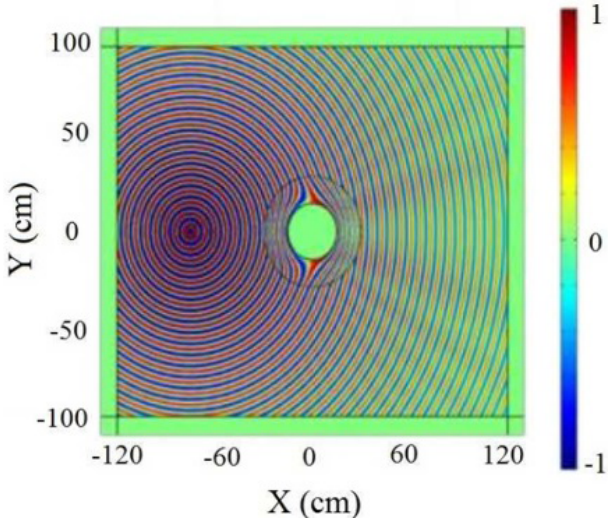

Figure 5. Simulation results when the incident wave is located outside the cloak at 5 GHz.

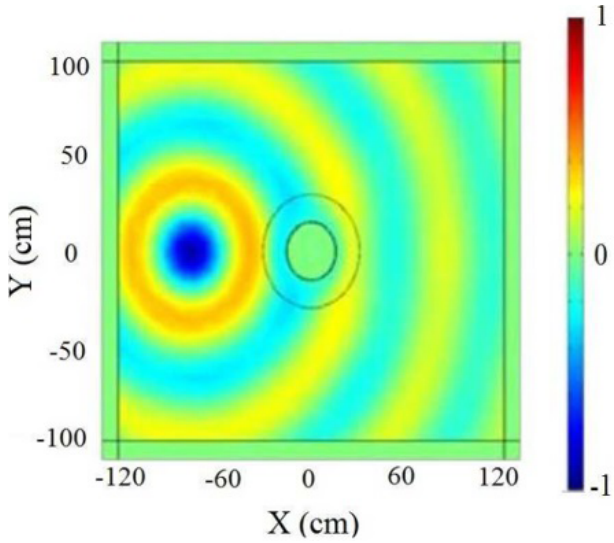

Figure 6. Simulation results when the incident wave is located outside the cloak at 0.5 GHz.

cloak smoothly bends the incident wave and guides it so that the wave propagates along the invisibility cloak. As a result, the conducting cylinder inside the cloak is not sensed, and no scattering field is produced by the cloak. In other words, the incident field behavior in the cloak presence is the same as when it propagates in the free space. In Figure 4, the simulation result for the linear line source located along the cloak axis is shown, and we can see that the incident waves do not leak from inside to outside the cloak. In order to investigate the cloak performance at different frequencies for the structure shown in Figure 2a, we simulate this structure at frequencies of 5 GHz and 0.5 GHz. Figures 5 and 6 represent the electric field profiles, when the electric line source is located outside the ideal cloak at these frequencies, respectively. According to these figures, we can see that the cloak shows acceptable behavior and performance. Nevertheless, at 0.5-GHz frequency, the incident wavelength is comparable to the cloak size, and the invisibility cloak performance can still be largely observed.

4. Conclusion

In this article, we used transformation optics to simplify the analysis and design of an invisibility cloak. To resolve the singularity in the boundary, we modified the constitutive tensors of the cloak. Great agreement was observed between the simulation results and the theoretical modeling. Moreover, when varying the incident wavelength, the cloak performance did not degrade considerably. As a result, our study shows that cloak behavior is not resonant.

References

[1] Cai W, Shalaev V. Optical Metamaterials: Fundamentals and Applications. New York, NY, USA: Springer, 2010.

[2] Leonhardt U. Optical conformal mapping. Science 2006; 312: 1777-1780.

[3] Pendry JB, Schurig D, Smith DR. Controlling electromagnetic fields. Science 2006; 312: 1780-1782.

[4] Yan W, Yan M, Ruan Z, Qiu M. Coordinate transformations make perfect invisibility cloaks with arbitrary shape. New J Phys 2008; 10: 1-13.

[5] Jiang WX, Chin JY, Li Z, Cheng Q, Liu R, Cui TJ. Analytical design of conformally invisible cloaks for arbitrarily shaped objects. Phys Rev E 2008; 77: 1-6.

[6] Nicolet A, Zolla F, Guenneau S. Electromagnetic analysis of cylindrical cloaks of an arbitrary cross section. Opt Lett 2008; 33: 1584-1586.

[7] Schurig D, Mock J, Justice B, Cummer S, Pendry J, Starr A, Smith D. Metamaterial electromagnetic cloak at microwave frequencies. Science 2006; 314: 977-980.

[8] Balanis CA. Advanced Engineering Electromagnetics. 2nd ed. Hoboken, NJ, USA: Wiley, 2012.

[9] Chew W. Waves and Fields in Inhomogeneous Media. New York, NY, USA: IEEE Press, 1995.

[10] Zhang B, Chen H, Wu B, Luo Y, Ran L, Kong JA. Response of a cylindrical invisibility cloak to electromagnetic waves. Phys Rev B 2007; 76: 12-15.

[11] Arslanagic S, Breinbjerg O. Electric-line-source illumination of a circular cylinder of lossless double-negative material: an investigation of near field, directivity, and radiation resistance. IEEE Anten Propag M 2006; 48: 38-54.